Constraints on the Upper Mantle Velocity Beneath the Yellow Sea, Eastern China

John J. Cipar
Earth Sciences Division (PL/GPE)
Phillips Laboratory

AFOSR Seismology Task 2309AP

Abstract. Detailed models of the crust and upper mantle are crucial for precise event location and computation of realistic synthetic seismograms for earthquake/explosion identification. However, such models are not available for most of the globe, including eastern China. In this report, data from the 1992 Yellow Sea earthquake is used to put constraints on the upper mantle velocity beneath the Yellow Sea and eastern China. The average velocity in the upper mantle is measured at 8.06 km/sec. Comparison of observed waveforms to synthetics suggests that the upper mantle P-wave velocity gradient is 0.0013 km./sec/km, with a higher gradient in the uppermost mantle just beneath the Moho. Availability of array data for a suite of events could be used to place strong constraints on the velocity structure.

Keywords: Seismology, Body wave propagation, Lithosphere and upper mantle, Asia

OBJECTIVE: To determine the crustal and upper mantle structure beneath eastern China

PRELIMINARY RESEARCH RESULTS:

Introduction

The details of the crust and upper mantle structure of eastern China have been measured in only a few places (Mangino and Ebel, 1992 and references cited therein). Mangino and Ebel (1992) used teleseismic receiver function observations to estimate the shear velocity of the crust at stations of the Chinese Digital Seismographic Network (CDSN). Nguyen and Hsu (1993) inverted surface wave group velocity dispersion curves from the 1992 Yellow Sea earthquake to obtain models for each of the CDSN stations. Cipar (1995) refined their focal mechanism using a grid search procedure and proposed a new crustal structure model for the Yellow Sea.

The 1992 Yellow Sea, China, Earthquake

A moderate earthquake occurred in the Yellow Sea off the coast of eastern China on 3 November 1992 at 17h 31m 23.7s. Coordinates are 35.328°N, 123.312°E; focal depth is 10 km, $m_b = 4.8$ (Preliminary Determination of Epicenters, November, 1992, Monthly Listing). Figure 1 shows the earthquake location and the locations of the CDSN stations used in this study (Table 1). Each station recorded the data in three pass bands: long-period (LH), broad-band (BH), and short-period (SH) (Peterson and Tilgner, 1985). Nguyen (1994) used CDSN surface wave observations to determine the mechanism of the 1992 Yellow Sea earthquake to be nearly strike-slip with a minor amount of dip-slip. His mechanism, shown in Figure 1, is consistent with first-motion measurements observed on CDSN short-period records. The fault plane has the parameters: strike = 15°, dip = 80°, and rake = 155°. He determined the source depth and seismic moment to be 9 km and 8.42×10^{22} dyne-cm, respectively.

In this report, I use the CDSN broadband data (the BH band) to place an additional constraint on the upper mantle velocity. The data set is less than ideal. The earthquake was of moderate magnitude located at sea far from the nearest seismic station, hence its location is imprecisely known and teleseismic observations are poor. In the context of nuclear treaty

Table 1. CDSN Station Information

Station Location	Latitude (°N)	Longitude (°E)	Elevation (m)	Delta (deg)	Distance (km)	Azimuth (deg)	Back Azimuth (deg)	
BJI	40.0403	116.1750	43.0	7.357	817.958	311.860	127.490	Beijing
ENH	30.2800	109.4975	487.0	12.661	1408.070	250.471	62.954	Enshi
HIA	49.2667	119.7417	610.0	14.175	1575.558	350.415	167.994	Hailar
HKC	22.3036	114.1719	0.0	15.238	1694.948	214.049	29.608	Hong Kong
KMI	25.1500	102.7500	1952.0	20.421	2271.258	245.854	55.375	Kunming
LZH	36.0867	103.8444	1560.0	15.836	1760.627	278.427	86.992	Lanzhou
MDJ	44.6164	129.5919	250.0	10.449	1161.622	25.507	209.557	Mudanjiang
SSE	31.0956	121.1867	10.0	4.581	509.467	203.475	22.310	Sheshan

monitoring, however, it is precisely these weak signals which will be of prime importance for discrimination of suspect events.

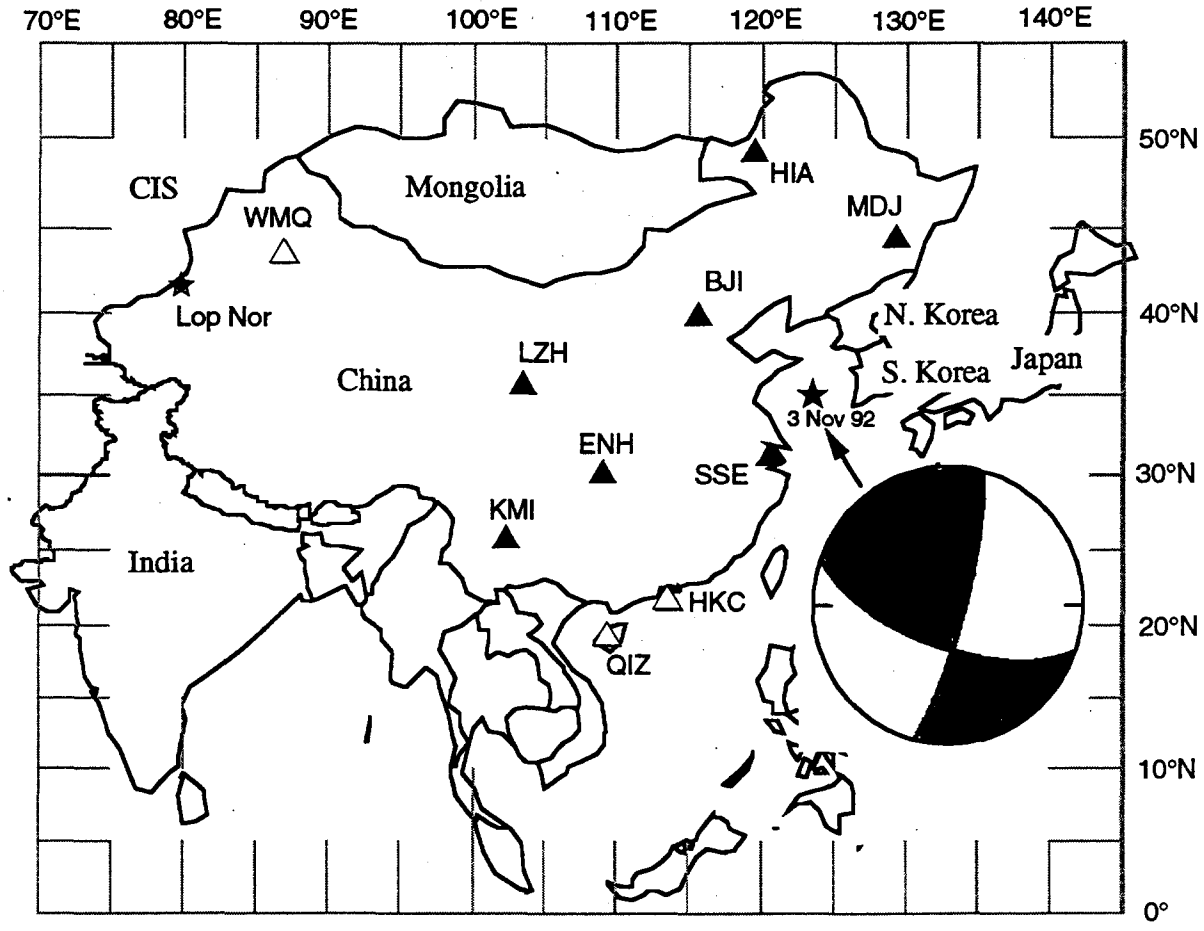

Figure 1. Map of the location of the Yellow Sea earthquake (star) and stations (filled triangles) used in this study. Open triangles denote other stations in the area. The inset shows the focal mechanism reported by Nguyen (1994); shaded quadrants are compressional.

Model for Crustal Structure

The starting velocity model for the crust was determined by Nguyen and Hsu (1993) as their MDJ model. The model was extended into the upper mantle using a constant velocity gradient. Although the attenuation was set rather high, the values are broadly consistent with previous measurements for the continental crust (Cheng and Mitchell, 1981). This starting model is designated A5 and is given in Table 2a.

Cipar (1995) used model A5 and the long-period (LH) channels at CDSN stations SSE, MDJ, BJI, HIA, LZH, and ENH to determine the focal mechanism by a gird search inversion procedure. The best fitting depth is 15 km, 6 km deeper than the depth determined by Nguyen (1994). The inferred mechanism is slightly different as well with a strike = 19°, dip = 90°, and rake = 173°. This mechanism is broadly consistent with the results reported by Nguyen (1994) especially given the fact that this inversion did not use any constraints such as P-wave polarities. It should be noted, however, that the focal mechanism reported by Nguyen (1994) produced rather large misfits at all source depths. The inferred source depth, 15 km, is well within the depths expected for a continental earthquake.

The focal mechanism grid search provides a source model that produces overall better agreement between observed and synthetic seismograms. Further improvement can be gained by modifying the crustal structure. Cipar (1995) tried several simple modifications of the MDJ path model (model A5). The most successful was dubbed A8 (Table 2b) in which the lower crustal velocity is reduced from 7.16 km/sec for A5 to 6.8 km/sec, and the Q reduced. The Pn velocity of A5 seems to be quite low compared to other continental regions, however, synthetics computed for higher Pn velocity values produced larger misfits than A8. Cipar (1995) adopted the Nguyen and Hsu (1993) Pn velocity as correct.

Upper Mantle Velocity

The broadband (BH band) data for the Yellow Sea earthquake are shown in record section format in Figure 2. The seismograms have been high-pass filtered to remove long-period noise and are plotted as trace normalized. Prominent phases are a clear Pn, especially at close distances, and Lg. A straight line fit to the first arrival observations at SSE, BJI, ENH, and HIA (see Figure 1), over the distance range 509 to 1575 km, indicates the average Pn velocity is 8.06 km/sec.

Broadband vertical seismograms for the two closest CDSN stations (SSE and BJI) are shown in the left panel of Figure 3, along with travel time curves computed for model A8 (Table 2b). We are looking at the first 60 seconds of record, that is, the P wave group. At these ranges, the first arrival is a strong, clear Pn. The travel time curves were computed for a surface source, whereas the earthquake occurred at 10 to 15 km depth. Nevertheless, the arrival times of the observed Pn phases closely match the theoretical curves in time. The A8 synthetics (right panel) were computed using the reflectivity method (Fuchs and Muller, 1971) for a 15-km deep source, hence the time discrepancy between travel time curves and synthetics. This implies that the travel times of the synthetics are early compared to the data. One obvious explanation is uncertainty in location and origin time. Alternatively, model A8 may be too fast relative to the true structure.

The synthetic waveforms provide a further constraint on the structure. One of the features of model A8 is high velocity gradients in the upper mantle which turn energy back to the surface, leading to strong first arrivals compared to later phases. The data, on the other hand, show strong first arrivals followed by a long coda, punctuated by several distinct phases. Unlike the A8 synthetics, however, the observed Pn phases are comparable in amplitude to later phases.

A range of models with constant gradients in the upper 160 km were tested by computing synthetics and comparing these to the observed seismograms. Synthetics for model A20 (Table 2c) with a gradient 0.0013 km/sec/km are shown in Figure 4. The Pn amplitude at BJI is comparable qualitatively to the observed record. The synthetic Pn at SSE,

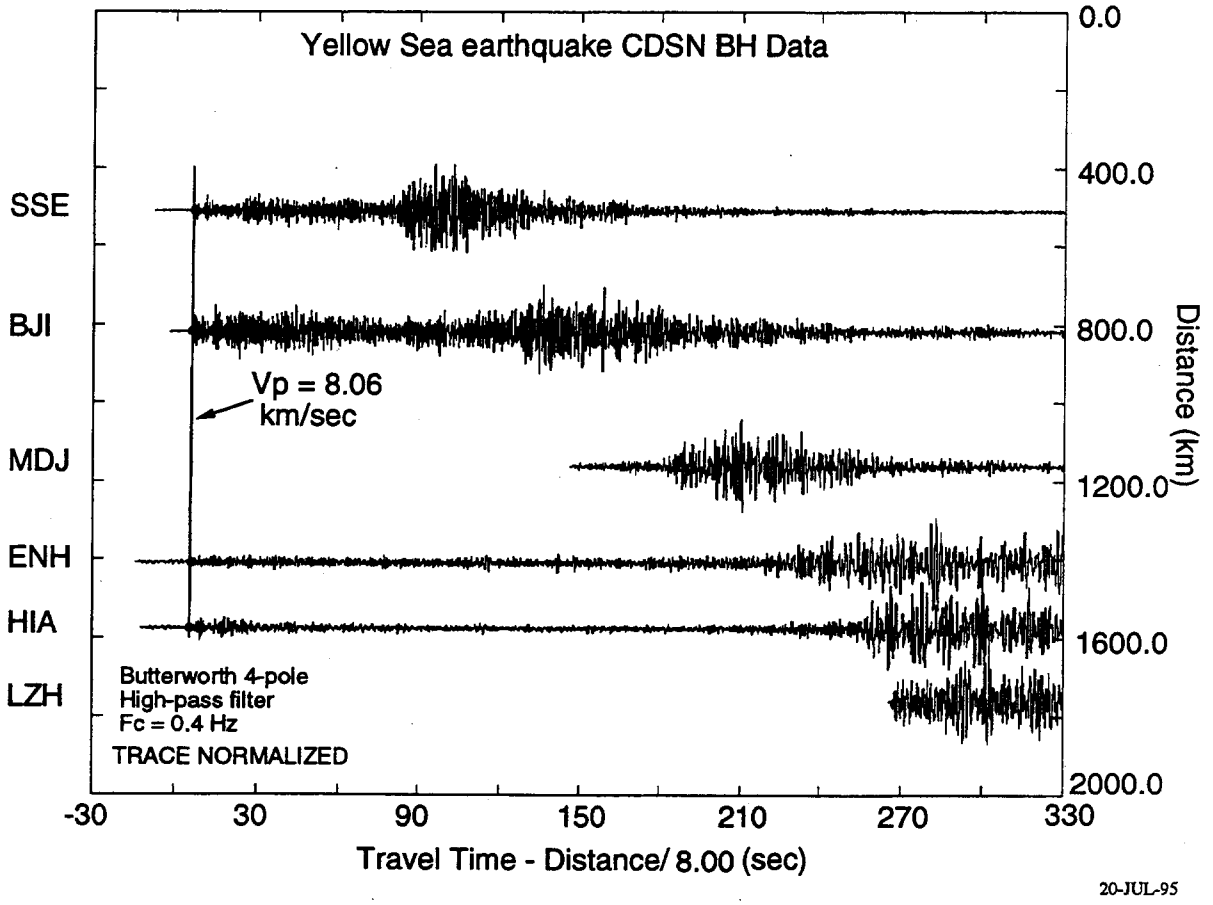

Figure 2. Broadband CDSN seismograms of the 1992 Yellow Sea earthquake displayed as trace normalized records. The seismograms have been high-passed filtered using a 4-pole Butterworth filter with a corner frequency of 0.4 Hz. The line marked 8.06 km/sec indicates the best fit straight line to measured first arrival times.

on the other hand, is too small compared to the observed Pn. The original MDJ model (A5) has a Moho velocity of 7.76 km/sec and we have already measured the average Pn velocity to be 8.06 km/sec. These observations suggest a strong gradient just below the Moho, which decreases with depth. Note that

Table 2. Crustal Models

Depth km	P-velocity km/s	Q_p	S-velocity km/s	Q_s	Density g/cm^3
		(a) Model A5			
0.0	4.06	200.0000	2.3500	100.0000	2.3300
1.0	4.06	200.0000	2.3500	100.0000	2.3300
1.0	5.42	1000.0000	3.1300	500.0000	2.5800
3.0	5.42	1000.0000	3.1300	500.0000	2.5800
3.0	6.16	1000.0000	3.5600	500.0000	2.7500
16.0	6.16	1000.0000	3.5600	500.0000	2.7500
16.0	7.16	1000.0000	4.1400	500.0000	3.0300
40.0	7.16	1000.0000	4.1400	500.0000	3.0300
40.0	7.76	1000.0000	4.4800	500.0000	3.2300
70.0	8.10	1000.0000	4.6767	500.0000	3.3203
100.0	8.20	1000.0000	4.7344	500.0000	3.3582
130.0	8.40	1000.0000	4.8499	500.0000	3.4339
160.0	8.50	1000.0000	4.9076	500.0000	3.4718
		(b) Model A8			
0.0	4.0600	50.0000	2.3500	25.0000	2.3300
1.0	4.0600	50.0000	2.3500	25.0000	2.3300
1.0	5.4200	100.0000	3.1300	50.0000	2.5800
3.0	5.4200	100.0000	3.1300	50.0000	2.5800
3.0	6.1600	525.0000	3.5600	263.0000	2.7500
16.0	6.1600	525.0000	3.5600	263.0000	2.7500
16.0	6.8000	525.0000	3.9261	263.0000	2.8278
40.0	6.8000	525.0000	3.9261	263.0000	2.8278
40.0	7.7600	525.0000	4.4800	263.0000	3.2300
70.0	8.1000	525.0000	4.6767	263.0000	3.3203
100.0	8.2000	525.0000	4.7344	263.0000	3.3582
130.0	8.4000	525.0000	4.8499	263.0000	3.4339
160.0	8.5000	525.0000	4.9076	263.0000	3.4718
		(c) Model A20 (same as A8 above 40 km)			
40.0	8.0000	525.0000	4.6200	263.0000	3.2300
70.0	8.0400	525.0000	4.6200	263.0000	3.3203
100.0	8.0800	525.0000	4.6300	263.0000	3.3582
130.0	8.1200	525.0000	4.6400	263.0000	3.4339
160.0	8.1600	525.0000	4.6415	263.0000	3.4718

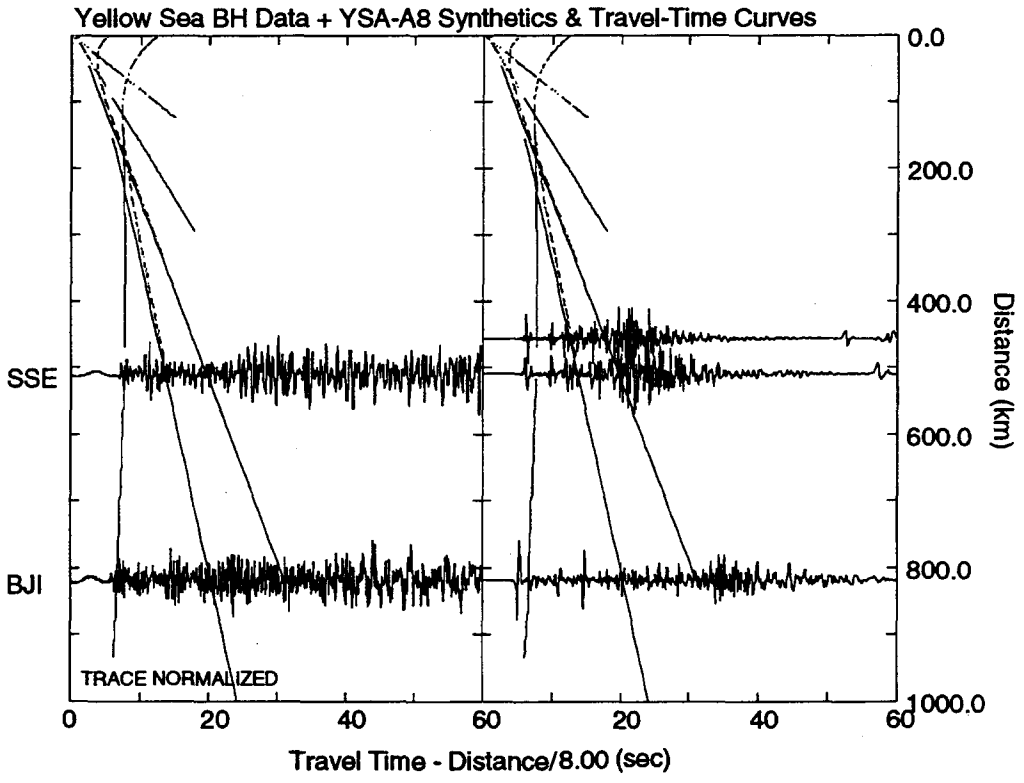

Figure 3. Broadband data of the Yellow Sea earthquake (left panel) and synthetic seismograms computed for model A8. Travel time curves are calculated for model A8 at zero source depth.

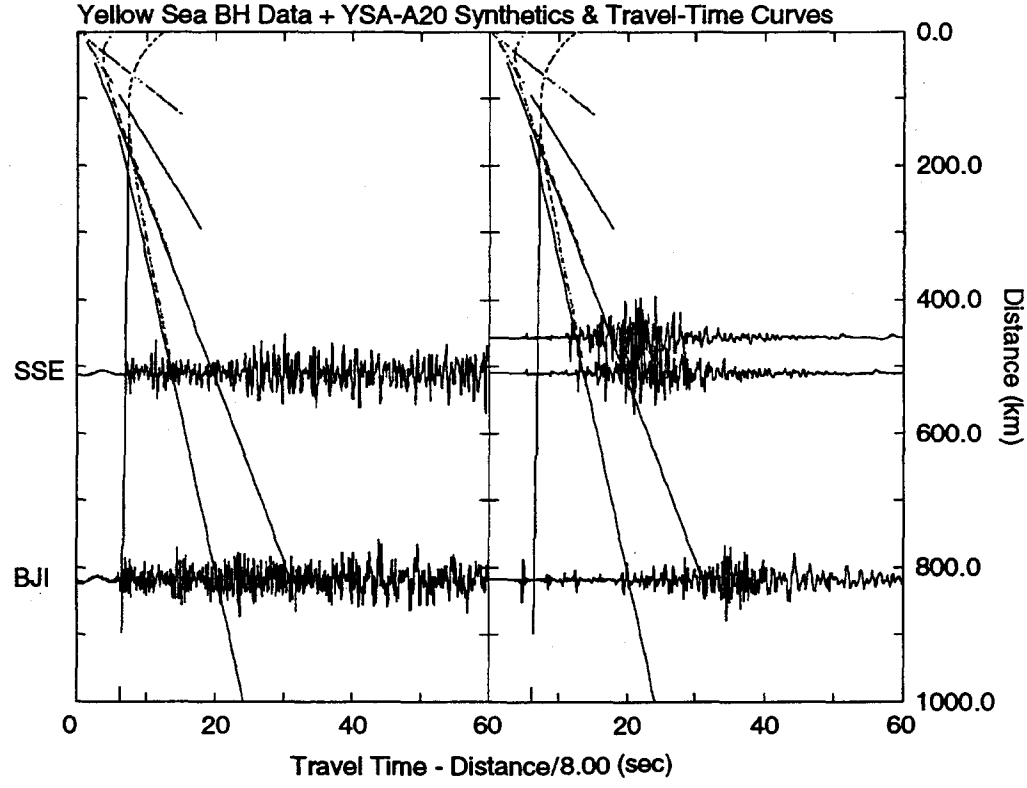

Figure 4. Broadband data of the Yellow Sea earthquake (left panel) and synthetic seismograms computed for model A20. Travel time curves are calculated for model A20.

20-JUL-95

the travel time curves for model A20 nearly overlay the observed Pn first arrivals.

CONCLUSIONS AND RECOMMENDATIONS:

The average upper mantle Pn velocity beneath the Yellow Sea and eastern China is 8.06 km/sec, determined using data from the 1992 Yellow Sea earthquake, and is consistent with other stable platform regions (Meissner, 1986). The P wave velocity gradient is 0.0013 km/sec/km, although it may be higher in the uppermost mantle just below the Moho. Array observations of a suite of events at a range of distances and azimuths could be invaluable in putting constraints on crust and upper mantle velocities.

Acknowledgments. I wish to thank Bao Nguyen and Vindell Hsu for providing the data for the Yellow Sea earthquake as well as their source and structure models in advance of publication. This work was supported under AFOSR Seismology Task 2309AP at the Earth Sciences Division, Phillips Laboratory.

References

Cheng, Chiung-Chuan and Brian J. Mitchell, Crustal Q structure in the United States from Multi-Mode Surface waves, *Bull. Seism. Soc. Am., 71,* 161-181 (February, 1981)

Cipar, John, A Grid Search Algorithm to Determine Earthquake Source Parameters - Application to the 1992 Yellow Sea, China, Earthquake, in press, PL-TR-95-2082

Fuchs, K. and G. Muller, Computation of Synthetic Seismograms with the Reflectivity Method and Comparison with Observations, *Geophys. J. Roy. Astron. Soc., 23,* 417-433 (1971)

Mangino, Stephen and John Ebel, The Receiver Structure Beneath the Chinese Digital Seismograph Network (CDSN) Stations: Preliminary Results, PL-TR-92-2149, Phillips Laboratory, Hanscom AFB, MA (30 April 1992) ADA256681

Meissner, Rolf, *The Continental Crust - A Geophysical Approach,* Academic Press, 1986, 426p.

Nguyen, Bao V. Surface-Wave Focal Mechanism of the 03 November 1992 Yellow-Sea Main Shock, *EoS (Trans. Am. Geophys. Union), 75,* 241, (April 19, 1994)

Nguyen, Bao V. and Vindell Hsu, Shear Path Structures from Inversions of Surface waves of the 03 November 1992 Yellow-Sea Main shock, *EoS (Trans. Am. Geophys. Union), 74,* 426 (Oct. 26, 1993)

Peterson, J. and E. E. Tilgner, Description and preliminary testing of the CDSN Seismic sensor systems, USGS Open File report 83-288, 37p., 1985.